

# IR-Active Phonons of Boron and Boron Carbide

H. Binnenbruck

II. Physikalisches Institut der Universität zu Köln\*

H. Werheit

FB 10/Physik der Gesamthochschule Duisburg

Z. Naturforsch. **34a**, 787–798 (1979); received May 3, 1979

The possible IR- and Raman-active phonons of  $\alpha$ -boron,  $\beta$ -boron, and boron carbide have been obtained by group theoretical methods. Reflectivity and absorption measurements in the spectral range from 10 to 1450  $\text{cm}^{-1}$  and a classical dispersion analysis yield the entire spectra of the anisotropic optical constants in the lattice vibration range of  $\beta$ -boron and beyond. From the reflectivity spectrum of boron carbide the resonance frequencies of the phonons and estimated values of their other characteristic values have been derived. The absorption spectrum of amorphous boron has been included in the discussion. — Certain frequency ranges can be attributed to vibrations of the icosahedra split in the crystal field. Single vibrations with  $E||c$  displaced to higher frequencies are attributed to the central atoms in the unit cells of  $\beta$ -boron and boron carbide. The phonon shift depending on temperature can be described by the Grüneisen shift. Three- and four-phonon processes are necessary to describe the temperature dependent damping constants of the lattice vibrations.

## Introduction

Concerning their crystalline structure the different crystalline modifications of boron and a number of its compounds, e.g. boron carbide, which is included in this work, are closely related. Main structure elements are metal-like bonded  $\text{B}_{12}$  icosahedra covalently bonded to neighbored icosahedra or to other structure elements. In a certain way amorphous boron can be included in this consideration, because it also contains  $\text{B}_{12}$  icosahedra and fragments of them, and therefore it has a more distinct narrow range order than many other amorphous semiconductors.

In earlier papers on the optical properties of these substances, apart from few exceptions [1–5], the main interest concerned the absorption edge and states in the band gap [6–9]. In the present work, group theoretical investigations on the phonons in  $\alpha$ -boron,  $\beta$ -boron and boron carbide are reported. The optical coefficients of  $\beta$ -boron and boron carbide in the lattice vibration range and beyond it, derived from reflectivity and absorption measurements, have been interpreted.

## Chemical Bond and Crystalline Structure

According to Muetterties [10] the chemical bond of the trivalent B atoms is determined by an excited state, which is characterized by four bond-

ing orbitals, only three of which are occupied by one electron, each. Such conditions lead to electron deficient structures with molecular-orbital bondings realized in crystals by preferred atom positions at the corners of polyhedra or related fragments. Thus the complex structures of the boron modifications and compounds become evident. Main structure element of the materials investigated in this paper is a nearly regular  $\text{B}_{12}$  icosahedron (Fig. 1) with twofold, threefold, and fivefold rotation axes and the inversion as symmetry elements [11, 12].

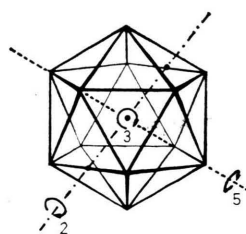


Fig. 1.  $\text{B}_{12}$  icosahedron with examples of 2-fold, 3-fold, and 5-fold rotation axes.

The icosahedron is kept together by thirteen bonding orbitals [13]. Besides there are twelve equivalent orbitals (s-p hybrids) pointing outward in the direction of the fivefold axes and leading to covalent bonds with other icosahedra or structure elements. Because of the overlap of all radial orbitals within the icosahedron the assumption of a nearest-neighbour interaction is not sufficient [14] and according to Weber and Thorpe [3] a metal-like bonding within the icosahedron can be assumed.

\* Present address DFVLR Köln

Reprint requests to Prof. Dr. H. Werheit, Fachbereich 10/Physik der Gesamthochschule Duisburg, Lotharstr. 65, 4100 Duisburg 1.

0340-4811 / 79 / 0700-0787 \$ 01.00/0



$\alpha$ -boron crystallizes in a rhombohedral lattice. The corners of the unit cell ( $a = 0.5057$  nm,  $\alpha = 58^\circ 4'$ ) are occupied by one icosahedron, each, being insignificantly distorted in the direction of the trigonal axis [15, 16]. The atoms on the edges of the rhombohedral cell are covalently bonded, whereas the equatorial atoms of the icosahedra form a three-center bond (cf. Figure 2).

The crystalline structure of boron carbide is very similar to that of  $\alpha$ -boron. Merely an additional three-atomic linear chain is arranged along the trigonal axis of the rhombohedral cell and widens the lattice ( $a = 0.519$  nm,  $\alpha = 65^\circ 18'$ ). The first structure conceptions were based on three C atoms in this chain ( $B_{12}C_3$ ), but recent investigations led

to the assumption of a C–B–C chain ( $B_{13}C_2$ ) (cf. e.g. [17, 18]). But boron carbide has a large continuous homogeneity range (atomic ratio B/C between about 9 and 2.4) [17, 19]. A statistical occupation of boron sites in the icosahedra seems possible [20]. The atoms at the outward positions of the chain are linked with the equatorial atoms of the icosahedra. Thus the bond strength is much greater than in  $\alpha$ -boron and leads to the very great hardness of boron carbide.

In the unit cell of  $\beta$ -rhombohedral boron ( $a = 1.01$  nm,  $\alpha = 65^\circ 17'$ ) the corners and the medium points of the edges are occupied by  $B_{12}$  icosahedra. On the major cell diagonal ( $c$ -axis in hexagonal description) two aggregates of three icosahedra, each, which are grown together at their surfaces, are arranged symmetrically to a single atom in the center of the cell [11]. The unit cell contains 105 atoms. The bonding between the structure elements is mainly covalent implying the great hardness of  $\beta$ -boron.

For group theoretical considerations a different description of the lattice structure of  $\beta$ -boron is more suitable: A central  $B_{12}$  icosahedron is linked with 12 half-icosahedra in the direction of its five-fold axes [16, 21]. This structure unit with 84 atoms

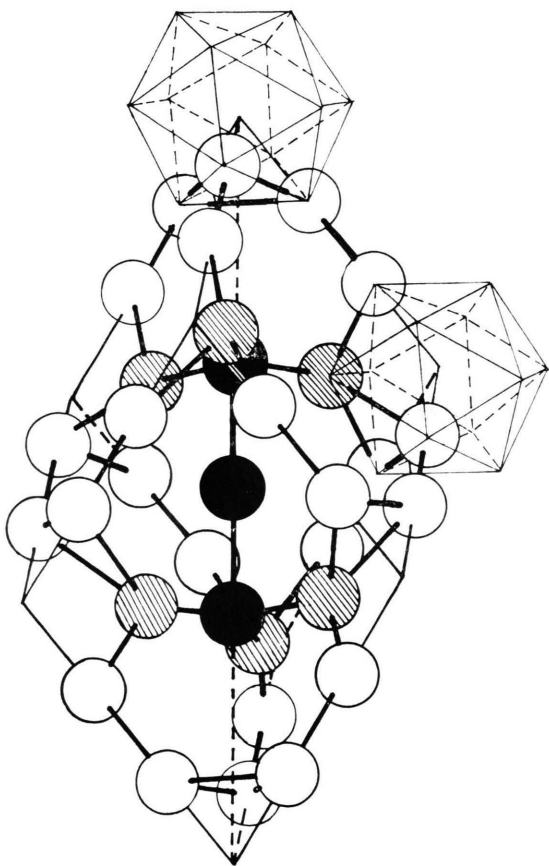


Fig. 2. Arrangement of the atoms in the unit cell of boron carbide and  $\alpha$ -boron (without the three-atomic chain in the major cell diagonal).

- atoms of the icosahedra, situated on the edges of the unit cell.
- ◐ equatorial atoms of the icosahedra forming multiple-center bonds.
- atoms of the three-atomic linear chain in boron carbide.

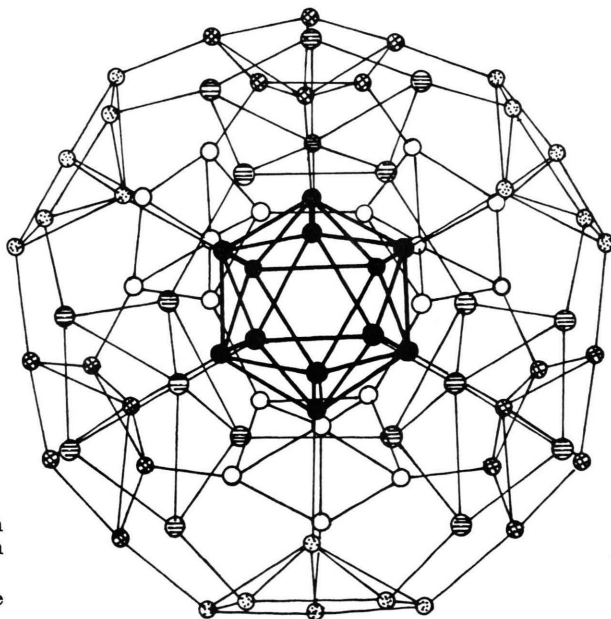


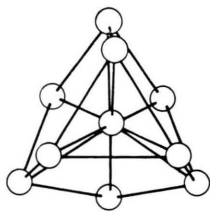
Fig. 3.  $B_{84}$  subunit of  $\beta$ -boron.

- atoms of the central icosahedron.
- ◐◐◐◐ atoms of half-icosahedra directing along the five-fold rotation axes of the central icosahedron.

Table 1. Symmetry elements  $\sigma$  with undisplaced atoms  $u(\sigma)$  of icosahedral systems.

$B_{12}$ (isolated icosahedron)	$\sigma$ $u(\sigma)$	$E$ 12	$C_5$ 2	$C_5^2$ 2	$i C_2$ 4
$\alpha$ -rhombohedral boron	$\sigma$ $u(\sigma)$	$E$ 12	$2C_3$ 0	$3C_2'$ 0	$i$ 0
$\beta$ -rhombohedral boron, $I_{84}$ subunit total	$2S_6$	84	0	0	0
	$\sigma_d$	21	3	1	3
	$3\sigma_d$	105	3	1	0
boron carbide	$u(\sigma)$	15	1	1	1
					1
					0
					7

and icosahedral symmetry (Fig. 3) is arranged at the corners of the unit cell in such a way that one of the three-fold axes coincides with the trigonal axis of the lattice. Then the half-icosahedra on the edges complete one another. The half-icosahedra directed into the interior of the unit cell are completed by two 10-atomic structure units consisting of three condensed caps of icosahedra (Figure 4). Together with the single atom in the center of the unit cell again 105 atoms result.

Fig. 4.  $B_{10}$  subunit of  $\beta$ -boron consisting of three condensed caps of icosahedra.

This kind of description shows the structural relationship between  $\beta$ -boron and boron carbide, in case the  $B_{12}$  icosahedron of boron carbide is assigned to the  $B_{84}$  unit of  $\beta$ -boron, and additionally on one hand the three-atomic chain and on the other hand the two condensed 10-atomic units together with the central atom are accounted for a kind of basis.

Deviations of this ideal structure depending on the preparation process are reported e.g. by Hoard et al. [22] and Runow [23]. Obviously  $\beta$ -boron has a low dislocation energy because of its electron deficient structure and its tendency to multiple-center bonds.

### Group Theoretical Determination of the IR- and Raman-active Vibrations

The normal modes have been obtained according to the usual procedure (cf. e.g. [25–27]). To

classify the  $q = 0$  phonons with respect to symmetry species, the representation of the point group in the vibration space has to be reduced to irreducible representations. Each normal mode ( $3 \cdot s$  dimensional vector;  $s$  = number of atoms in the unit cell) is positioned in one of the irreducible subspaces  $U_i$ . The number of the normal modes belonging to the  $i$ th symmetry species is obtained from the dimensionality  $\text{Dim } U_i$ . Considering the normal degeneracy caused by symmetry,  $\text{Dim } U_i$  has to be divided by the dimensionality of the  $i$ -th irreducible representation thus yielding the number  $n_i$  of the symmetry species, which normally have different frequencies.

The number  $u(\sigma)$  of the undisplaced atoms belonging to different symmetry elements  $\sigma$  have been obtained from structure models of the lattices (Table 1) taking the icosahedra as regular. In the case of  $\beta$ -boron the undisplaced atoms  $u_i$  of the subunits have been taken separately. From these values, together with the characters of the point groups  $I_h$  and  $\bar{3}m$  taken from their character tables [25, 26],  $\text{Dim } U_i$  and  $n_i$  have been calculated (Table 2 and 3). Taking the selection rules into account and eliminating the translation as displacement of the lattice as a whole, the possible

Table 2.  
 $B_{12}$  icosahedron.

Vibration species	$\text{Dim } U_i$	$n_i$
$A_g$	1	1
$A_u$	0	0
$F_{1g}$	3	1
$F_{1u}$	6	2
$F_{2g}$	0	0
$F_{2u}$	3	1
$G_g$	4	1
$G_u$	4	1
$H_g$	10	2
$H_u$	5	1

Table 3.

Vibration species	$\alpha$ -boron Dim $U_i$ $n_i$		$\beta$ -boron Dim $U_i$ $n_i$		Boron carbide Dim $U_i$ $n_i$	
A <sub>1g</sub>	4	4	31	31	5	5
A <sub>2g</sub>	2	2	21	21	2	2
E <sub>g</sub>	12	6	104	52	14	7
A <sub>1u</sub>	2	2	21	21	2	2
A <sub>2u</sub>	4	4	32	32	6	6
E <sub>u</sub>	12	6	106	53	16	8

IR- and Raman-active vibrations have been derived and attributed to the dielectric principal axes of the crystals (Table 4).

Additional group theoretical considerations yield valuable information concerning the relation between the vibration spectra of the crystals and vibration modes of the icosahedron. When the icosahedron is located in the crystal field of the rhombohedral lattice, its symmetry is reduced. The icosahedral group becomes reduced to the point group and the degeneracy is partly lifted. The splitting can be determined by reducing the icosahedral group with respect to the point group  $\bar{3}m$ . As the sum of the characters of both representations correspond, the splitting can be obtained [27] from the possible combinations between the point group  $\bar{3}m$  and the subgroup  $\bar{3}m$  of the icosahedral group (Table 5). From this table can be seen that the following IR- and Raman-active phonons of the crystals result from split icosahedral modes:

IR-active: 3 A<sub>2u</sub> ( $E \parallel c$ ) 5 E<sub>u</sub> ( $E \perp c$ )

Raman-active: 4 A<sub>1u</sub> ( $E \parallel c$ ) 6 E<sub>g</sub> ( $E \perp c$ )

Consequently a comparison with the results in Table 4 shows e.g. that in  $\alpha$ -boron no vibrations of

A <sub>g</sub>	→ A <sub>1g</sub>
F <sub>1g</sub>	→ A <sub>2g</sub> + E <sub>g</sub>
F <sub>1u</sub>	→ A <sub>2u</sub> + E <sub>u</sub>
F <sub>2g</sub>	→ A <sub>2g</sub> + E <sub>g</sub>
F <sub>2u</sub>	→ A <sub>2u</sub> + E <sub>u</sub>
G <sub>g</sub>	→ A <sub>1g</sub> + A <sub>2g</sub> + E <sub>u</sub>
2 H <sub>g</sub>	→ 2 A <sub>1g</sub> + 4 E <sub>g</sub>
H <sub>u</sub>	→ A <sub>1u</sub> + 2 E <sub>g</sub>

Table 5. Splitting of the vibration modes of the icosahedron in the rhombohedral crystal field.

other kind than split vibrations of the icosahedron are to be expected.

### Sample Material

Experimental investigations have been performed on the vibration spectra of crystalline  $\beta$ -boron, crystalline boron carbide, and amorphous boron. The sample material was of very different quality.

#### a) $\beta$ -Boron

The samples have been cut from hyper-pure single crystals (Wacker-Chemie, Munich). Typical impurity analysis according to the producer: C: 50–100 ppm; Si, Ca, Cu, Mg: 1 ppm (cf. [9]). Laue patterns obtained for orientation have split reflexes. X-ray investigations led to the assumption of stacking faults and twin structures [24]. Details of the sample preparation are given in [24].

#### b) Boron Carbide

Different material of industrial production has been supplied by the Elektroschmelzwerk Kempten: aa) Coarse crystalline, porous lumps. Typical analysis: B: 79.3 weight%; C: 20.5%; B<sub>2</sub>O<sub>3</sub>: 0.1%; Fe: 0.05%; Al, Ca: < 0.01%; Si: not detectable. Qualitative measurements of the magnetic susceptibility point at low ferromagnetic impurities [28].

Table 4. Optical phonons of icosahedral systems.

System	Point group	Atoms per unit cell	IR-active modes		Raman-active modes	
			theor.	exp.	theor.	exp.
B <sub>12</sub> (isolated icosahedron)	I <sub>h</sub>	12	1 F <sub>u</sub>		1 A <sub>g</sub> 2 H <sub>g</sub>	
B $\alpha$ -rhom.	$\bar{3}m$	12	3 A <sub>2u</sub> 5 E <sub>u</sub>	2 [1]	4 A <sub>1g</sub> 6 E <sub>g</sub>	9 [4]
B $\beta$ -rhom.	$\bar{3}m$	105	31 A <sub>2u</sub> 52 E <sub>u</sub>	24 25	31 A <sub>1g</sub> 52 E <sub>g</sub>	10 (broad) [2]
B <sub>12</sub> C <sub>3</sub>	$\bar{3}m$	15	5 A <sub>2u</sub> 7 E <sub>u</sub>	9 + (3)	5 A <sub>1g</sub> 7 E <sub>g</sub>	



bb) Rod hot pressed in a graphite mold. Typical analysis: B: 78 weight%; B + C: 99%; graphitic C: 1%; other data like those above. Qualitative measurements of the magnetic susceptibility point at greater concentrations of ferromagnetic impurities [28].

cc) Single crystals originated by chance during the technical production in rodlike form (side plane  $\parallel c$ ) and platelike form (surface  $\perp c$ ). The orientation has been confirmed by Laue patterns. Split reflexes similar to those of  $\beta$ -boron have been found. The B/C ratio of the samples is not known. But essential deviations from the compound  $B_{12}C_3$  are not expected, as this composition is aimed at. According to recent investigations on defined samples the phonon energies are slightly dependent on the composition [20].

The polycrystalline samples have been cut by use of a diamond saw, and lapped and polished with diamond paste of different grain size. They have not been etched since a polishing etching solution is not known, but because of the great hardness no essential Beilby layer is to be expected.

#### c) Amorphous Boron

The samples have been evaporated by electron bombardement and deposited on polyethylene foils in vacuum of about  $10^{-5}$  mbar. Impurity data of the films are not known.

### Methods of Measurement and Analysis

Reflectivity and partly absorption measurements have been performed in the range from 10 to  $1450\text{ cm}^{-1}$ . Depending on the spectral range a Fourier-spectrometer ( $10\text{--}100\text{ cm}^{-1}$ ), a FIR-lattice-spectrometer (Perkin-Elmer 301;  $100\text{--}700\text{ cm}^{-1}$ ) and a prism-spectrometer with Leiss double monochromator ( $700\text{--}1400\text{ cm}^{-1}$ ) have been used. Deviations from normal incidence in the reflectivity measurements have been corrected by use of the Fresnel formulae. The transmission measurements on amorphous boron have been made with a double-beam lattice spectrometer.

The spectra have been analyzed by use of the classical dispersion theory, and if necessary the Drude theory for free carriers has been applied. Thus the complex dielectric constant can be described by the superposition of suitably chosen

dispersion oscillators (cf. e.g. [29]):

$$\varepsilon(\nu) = \varepsilon_{\infty} + \sum_j \frac{\Delta\varepsilon_j}{1 - (\nu/\nu_{j0})^2 - i(\gamma/\nu_{j0})(\nu/\nu_{j0})},$$

$\varepsilon_{\infty}$  optical dielectric constant (contribution of bonded electrons),

$\Delta\varepsilon_j$  oscillator strength (contribution of the  $j$ -th oscillator),

$\nu$  frequency in wave-numbers ( $\text{cm}^{-1}$ ),

$\nu_j$  resonance frequency of the sustained oscillators,

$\gamma$  frequency independent damping constant.

Free carriers can be characterized by the plasma resonance frequency  $\omega_p = (Ne^2/m\varepsilon_0\varepsilon)^{1/2}$  and the collision frequency  $\omega_{\tau} = 1/\tau$ . The influence on the dielectric constant (cf. e.g. [30]) is given by

$$\varepsilon(\omega) = \varepsilon_{\infty} - \frac{\omega_p^2}{\omega^2 + \omega_{\tau}^2} - i \frac{\omega_{\tau}}{\omega} \frac{\omega_p^2}{\omega^2 + \omega_{\tau}^2}.$$

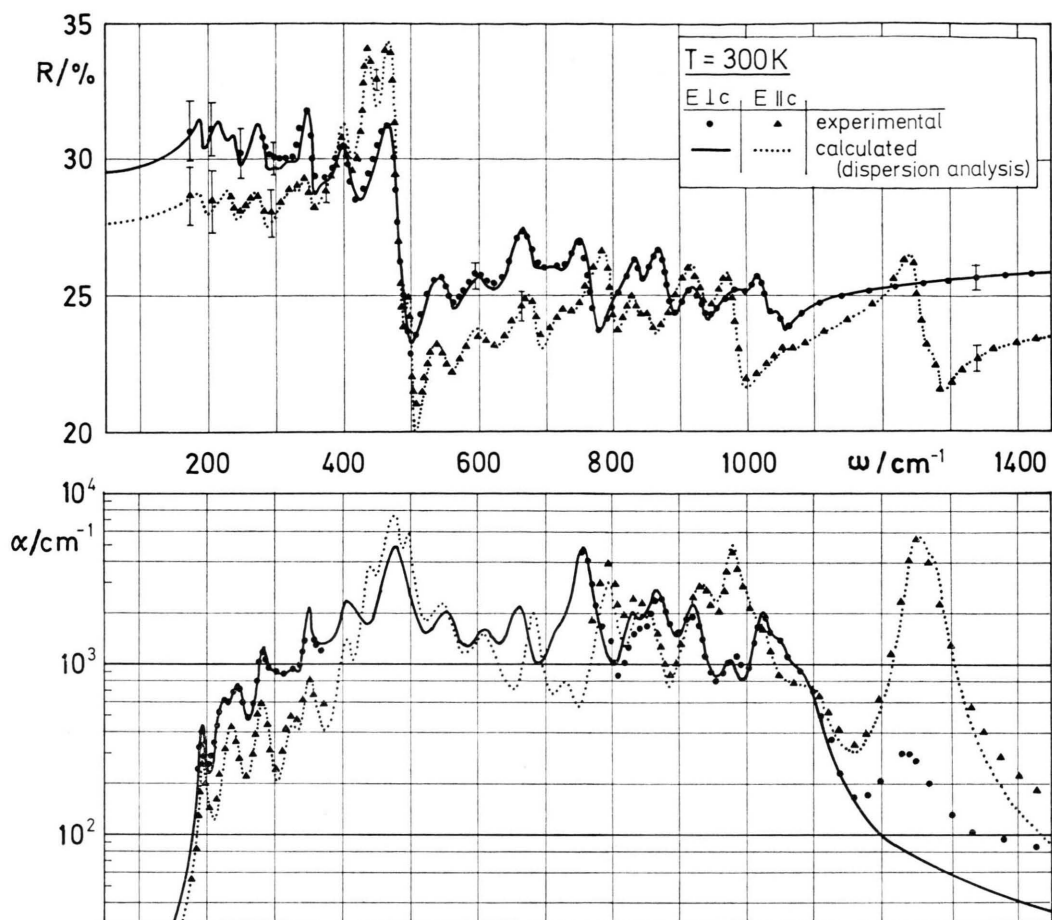
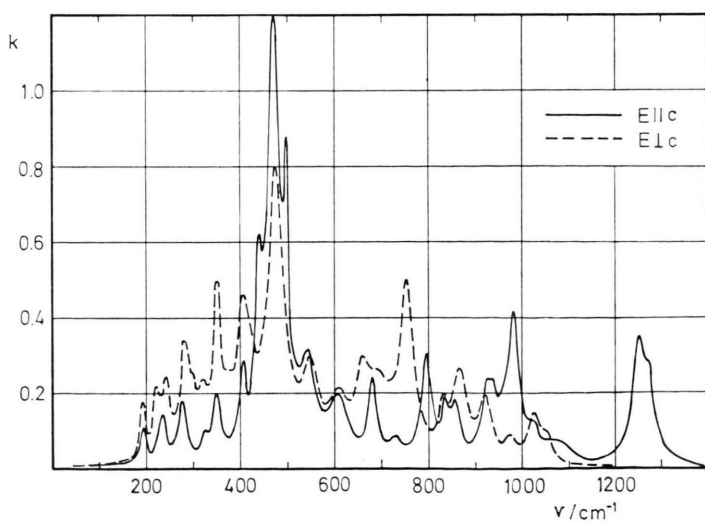
From the dielectric constant the optical constants can be calculated in the usual way. The required parameters have been obtained from the measured spectra and then successively improved. At first this representation of the measured spectra is only a formal procedure. A physical interpretation on the base of IR-active vibrations requires additional conditions:

- 1) The number of the oscillators must not exceed the group theoretically permissible maximum.
- 2) Multi-phonon processes are to be excluded, because e.g. in alkali halides [31] they require a description by a frequency dependent damping constant.

### Results

#### a) $\beta$ -Boron

Reflectivity and absorption coefficient of  $\beta$ -boron are shown in Figure 5. The measured values are well represented by the dispersion analysis. Deviations in the range of great wave numbers are caused by the following reasons: The dispersion analysis neglects that the absorption of the strong band at  $1260\text{ cm}^{-1}$  with  $E \parallel c$  appears also  $\perp c$ , probably because of the structural imperfections. Additionally the unstructured absorption at higher wave numbers up to about  $2500\text{ cm}^{-1}$  [9], which obviously can be attributed to multi-phonon processes, has not been taken into account.

Fig. 5. Absorption coefficient and reflectivity of  $\beta$ -boron.Fig. 6. Absorption index of  $\beta$ -boron.

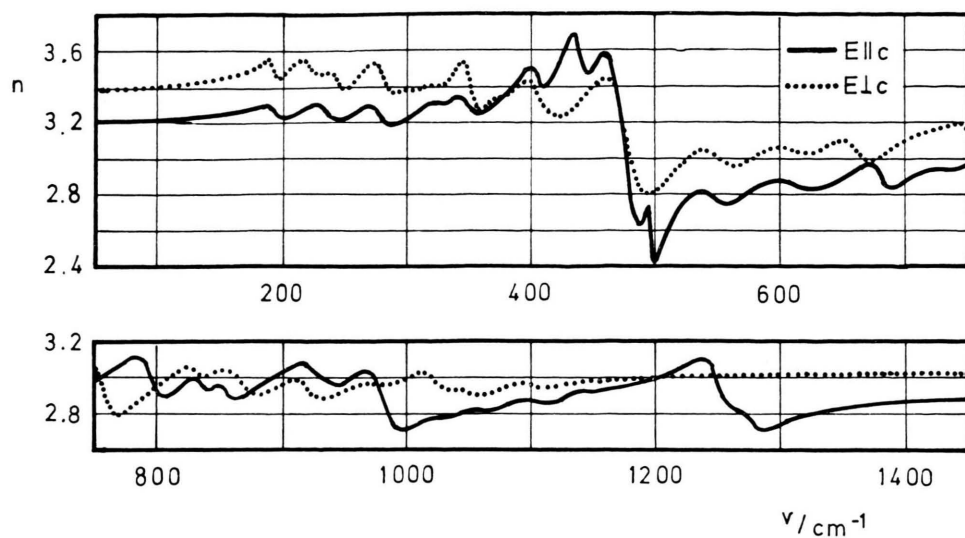
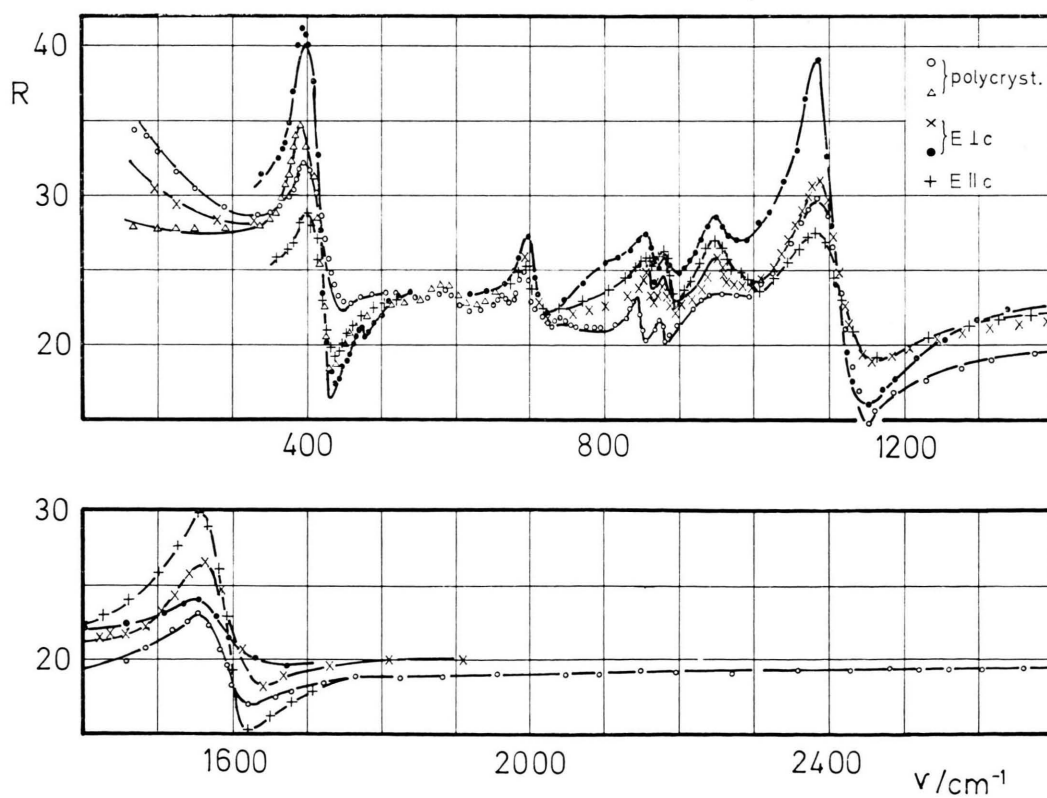
Fig. 7. Refractive index of  $\beta$ -boron.

Fig. 8. Reflectivity of boron carbide.

Table 6. Properties of the IR-active lattice vibration frequencies of  $\beta$ -boron (obtained from the dispersion analysis).

Symmetry species $A_{2u}$ ( $E \parallel c$ )			Symmetry species $E_u$ ( $E \perp c$ )		
$\nu_0$ [cm <sup>-1</sup> ]	$\Delta\epsilon$	$\gamma$ [cm <sup>-1</sup> ]	$\nu_0$ [cm <sup>-1</sup> ]	$\Delta\epsilon$	$\gamma$ [cm <sup>-1</sup> ]
1275	0.022	30	1090	0.005	30
1250	0.044	30	1050	0.010	30
1110	0.005	30	1030	0.010	30
1090	0.005	30	1025	0.030	30
1025	0.008	30	980	0.010	30
980	0.080	35	920	0.030	30
940	0.010	20	865	0.060	30
925	0.033	30	830	0.015	20
855	0.017	20	755	0.100	30
835	0.017	20	725	0.035	50
795	0.055	26	690	0.065	50
730	0.010	25	660	0.050	30
680	0.033	20	610	0.070	50
610	0.070	50	550	0.090	40
545	0.090	40	475	0.400	40
497	0.020	5	420	0.100	40
472	0.550	35	405	0.100	25
440	0.090	15	375	0.100	40
405	0.050	15	351	0.100	15
349	0.060	20	322.5	0.075	30
325	0.015	15	300	0.075	30
278	0.070	20	280	0.120	20
236	0.070	20	243	0.100	20
193	0.050	15	225	0.100	20
			192	0.050	10

Resonance frequencies, oscillator strengths and damping constants of the phonons according to the dispersion analysis are listed in Table 6. The spectra of absorption index and refractive index based on these data are plotted in Figs 6. and 7.

In the spectral range from 10 to 100 cm<sup>-1</sup>  $\beta$ -boron is transparent. At room temperature no absorption of free carriers was detectable in a sample of 95  $\mu$ m thickness. Therefore it was possible to obtain exact values of the medium refractive index and the dielectric constant from the interferences in the transmission spectrum:

$$E \parallel c: \quad \bar{n} = 3.40 \pm 0.05, \quad \bar{\epsilon} = 11.55 \pm 0.30,$$

$$E \perp c: \quad \bar{n} = 3.20 \pm 0.05, \quad \bar{\epsilon} = 10.24 \pm 0.30.$$

In the dispersion analysis these values and the refractive index in the range  $> 1450$  cm<sup>-1</sup> [32] obtained from interferences, too, have been taken into account. The resulting average dielectric constant

$$\bar{\epsilon} = 10.66 \pm 0.30$$

agrees very well with the static dielectric constant of polycrystalline  $\beta$ -boron ( $\epsilon_{stat} = 10.6 \pm 0.2$ ) reported by Lagrenaudie [33] and thus no essential dispersion processes in the spectral range  $< 10$  cm<sup>-1</sup> are to be expected.

#### b) Boron Carbide

All the samples were only suitable for reflectivity measurements. Because of the non-ideal surfaces the measured values are probably somewhat too low and differ from sample to sample. The small size of the single crystals led to an unfavourable signal to noise ratio and therefore it prevented measurements in the boundary ranges of the spectrometers. Figure 8 shows the experimental results. In the case of boron carbide the dispersion analysis was partly restricted to limited subranges. The medium oscillator strengths are summarized in Table 7.

The Drude frequencies of the different samples vary in the ranges

$$\omega_p = 2 \dots 3.1 \cdot 10^{14} \text{ s}^{-1},$$

$$\omega_\tau = 1.5 \dots 8 \cdot 10^{14} \text{ s}^{-1}.$$

Using the density of free holes ( $N_h = 4 \dots 9 \cdot 10^{25}$  m<sup>-3</sup>) obtained from Hall-effect measurements on comparable material by Geist et al. [34], the effective mass of the holes

$$m_h = 3 \dots 5 m_0$$

results in agreement with the estimation of Geist et al. [34] derived from Hall-effect and conductivity data. Taking into account recent investigations of Werheit and de Groot [35] on the electrical conductivity and the thermoelectric power of boron

Table 7. Medium oscillator strengths  $\Delta\epsilon$  of the phonons in boron carbide (uncertain values in brackets).

Wave number [cm <sup>-1</sup> ]	Polycryst. material	Single crystals		Prevailing symmetry type
		$E \parallel c$	$E \perp c$	
1580	0.15	0.45	0.12	$A_{2u}$ $E_u$
1090	0.35	0.25	0.5	
(980)	—	—	—	$A_{2u}$
870	0.02	0.08	0.06	
873	0.01	0.04	0.02	
845	0.02	0.03	0.01	
700	0.07	0.05	0.04	
(660)	—	—	—	$E_u$
582	0.06	—	0.20	
(530)	—	—	—	$E_u$
475	—	—	—	
390	0.6	0.35	0.60	



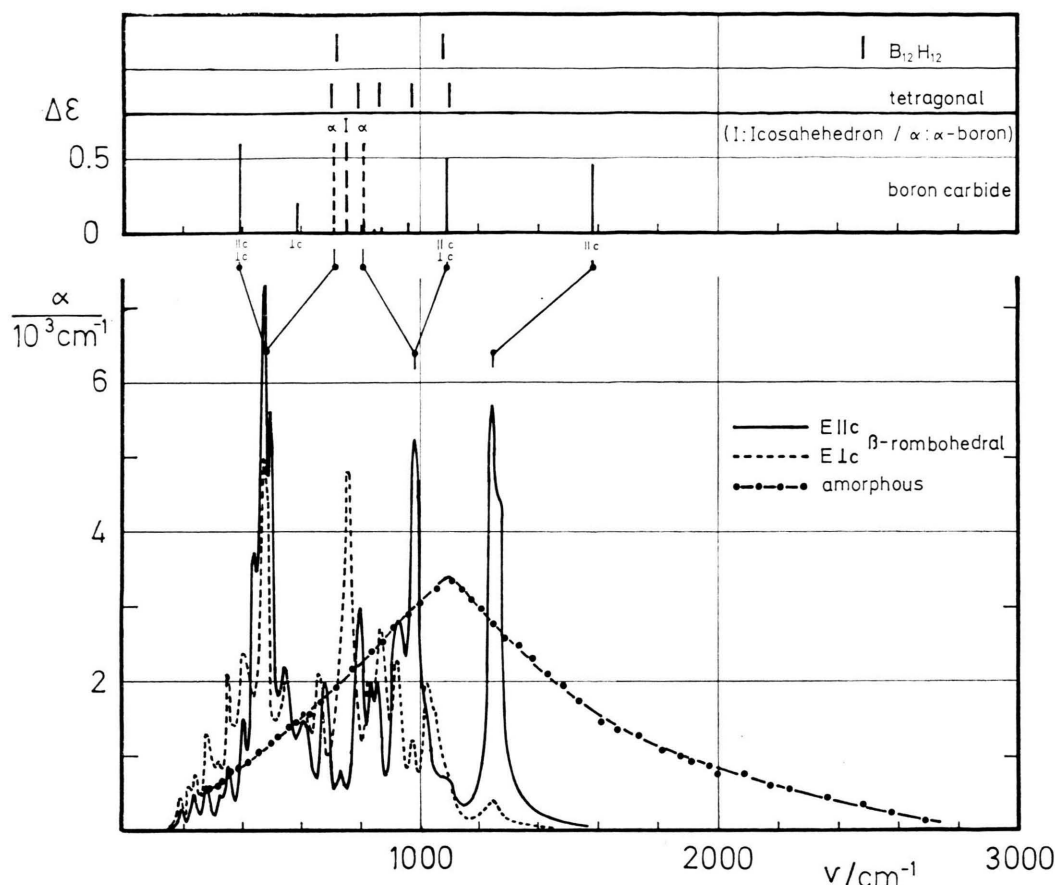


Fig. 9. Comparison of the absorption of icosahedral boron systems (data on  $\alpha$ -boron, tetragonalboron, and  $B_{12}H_{12}$  obtained from [1] and references therein).

carbide with defined composition, it seems that these values cannot be attributed to free holes in the extended states of the valence band but to the conduction in more or less localized states in the band gap.

### c) Amorphous Boron

The absorption coefficient (plotted in Fig. 9) has been calculated from the transmission of films of different thickness. As a double-beam spectrometer has been used, the absorption of the supporting foils could be eliminated by an uncoated foil in the reference beam. The absorption is rather low in comparison to the range of electronic transitions. This may be the reason why other authors (e.g. [36]) did not succeed in measuring the absorption in the lattice vibration range of amorphous boron when films of insufficient thickness were used.

### Interpretation of the Phonon Spectra

The inter-icosahedral and the intra-icosahedral bonds are of comparable strengths, which results from the comparable interatomic distances in both cases. Therefore contrary to molecular crystals no distinct spectral separation between interior and exterior vibrations of these structure elements occurs. In the crystals the icosahedra are strongly coupled and thus their vibration modes split. The rate of this splitting depends strongly on the bond strength, which macroscopically appears in the hardness of the crystals increasing from  $\alpha$ -boron via  $\beta$ -boron to boron carbide.

According to Becher [1] in the rhombohedral lattice of  $\alpha$ -boron the vibration mode of the icosahedron ( $750\text{ cm}^{-1}$ ) splits nearly symmetrically into two lines at  $710$  and  $810\text{ cm}^{-1}$ . Because of the similarity of the lattice structure of boron carbide

corresponding phonon lines are to be expected, but of course more strongly split because of the stronger bond strength. Therefore it seems to be reasonable to interpret the phonons at 390 and 1090  $\text{cm}^{-1}$  in this way (Figure 9).

Both lines appear  $\parallel c$  as well as  $\perp c$  though prevailing  $\perp c$ . Consequently they cannot be uniquely attributed to the symmetry species  $A_{2u}$  or  $E_u$ .

According to Hoard and Hughes [16] negative charge is transferred from the central atom of the three-atomic chain to the icosahedron. Consequently a dipole moment arises and thus a distinct phonon band  $\parallel c$  is to be expected. Because of the small mass the resonance frequency of this phonon should be high. From the group theoretical considerations results that this is one of the two vibrations of the species  $A_{2u}$  which do not result from split icosahedral modes. The phonon line at 1480  $\text{cm}^{-1}$  fulfils those conditions.

The structural relationship between  $\beta$ -boron and boron carbide has already been mentioned. Trying a subdivision of the phonon spectrum of  $\beta$ -boron corresponding to that one of boron carbide (cp. Fig. 9), again a limited frequency range, occupied by phonons of both species, is to be found. This is limited by phonons of great oscillator strengths (cf. Fig. 7) at about 470 and 980  $\text{cm}^{-1}$ . On account of the smaller bonding strengths in  $\beta$ -boron the spectral split is of course smaller than in boron carbide. The greater phonon density in this range in comparison to boron carbide is explained by the group theoretical analysis.

In  $\beta$ -boron, too, a strong vibration  $\parallel c$  significantly displaced to higher frequencies is to be found, which in analogy to boron carbide is attributed to the single atom in the center of the unit cell.

The extent of the frequency range of the split vibration modes of the icosahedron in  $\beta$ -boron agrees with the estimation of Weber and Thorpe [3], but it is distinctly displaced to lower frequencies.

The above interpreted low frequency limit of the split icosahedral modes is followed by several distinct vibrations towards lower frequencies. It seems to be reasonable to assign the range  $\leq 400$   $\text{cm}^{-1}$  to vibrations of greater structural units. This assumption is supported by the following considerations: According to Runow [23] the unit cell of  $\beta$ -boron can be imagined as approximately assembled out of eight unit cells of  $\alpha$ -boron.

Consequently the Brillouin zone of  $\beta$ -boron can be approximately be obtained by bisecting the Brillouin zone of  $\alpha$ -boron (Figure 10). Then the

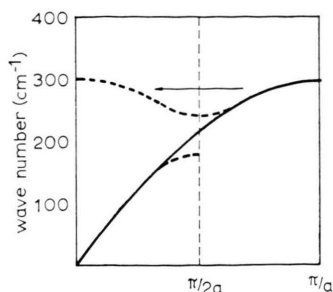


Fig. 10. Doubling of the periodicity of the Brillouin zone of  $\alpha$ -boron by the transformation to  $\beta$ -boron ( $a = 0.506$  nm).

acoustic phonon cutoff of  $\alpha$ -boron (300  $\text{cm}^{-1}$ , according to Slack et al. [37]) is transferred into an optical vibration in the center of the Brillouin zone of  $\beta$ -boron, whose acoustic phonon cutoff is at 130  $\text{cm}^{-1}$  [37]. As the quoted data obtained from elastic properties are mean values, it can be largely excluded that split icosahedral modes occur in the range from 200 to 400  $\text{cm}^{-1}$ . An additional argument is yielded by the absorption spectrum of amorphous boron, whose narrow range order (icosahedra and related fragments) is mainly retained (Katada [38]), whereas the crystalline long range order is destroyed. The absorption maximum, which is to be attributed to the vibrations of the narrow range order, is doubtlessly positioned in the range of the high frequency vibrations of crystalline boron.

Generally it can be stated that the number of experimentally found phonons is smaller than permitted by group theory (Table 4). This may be caused e.g. by the following reasons:

- 1) accidental degeneracy,
- 2) too small effective charges of missed modes.

Cases of accidental degeneracy are very probable in the case of  $\beta$ -boron, because a great number of symmetry-permitted modes is concentrated in a narrow spectral range; the medium frequency interval per vibration is comparable to the medium damping constant (Table 6). The oscillator strengths (Tables 6 and 7) are small in comparison to the IR-active vibrations of many other crystals. This can be explained by the strong, mainly covalent bonding

with small distortion of the bonding orbitals and the small effective charges related.

The strong damping of the oscillators may be mainly caused by isotope effects (ratio  $^{10}\text{B}/^{11}\text{B} \approx 20/80$ ) and lattice defects.

### Temperature Dependence of Phonon Frequencies and Damping Constants of $\beta$ -boron

While the phonons in  $\beta$ -boron shift to lower frequencies with increasing temperature, the oscillator strengths remain constant within the accuracy of measurement and the damping constants increase. This behaviour has been analyzed quantitatively on some phonons by using new reflectivity measurements as well as later absorption measurements of Jaumann and Werheit [39], which now can be attributed to special symmetry types applying the present group theoretical results.

The shift of the phonon frequencies can mainly be attributed to two contributions:

$$d\omega_i = (\partial\omega_i/\partial V)_T dV + (\partial\omega_i/\partial T)_V dT.$$

Herein the first term describes the thermal dilatation of the lattice and the second one the contribution of the temperature dependent anharmonicity of the bond. According to [40, 41] the second term increases with  $T^2$  at high temperatures, but, as will be seen, in the case of  $\beta$ -boron, this is not detectable in the investigated temperature range in comparison to the first term.

By use of data on the macroscopic behaviour of  $\beta$ -boron obtained from literature (molar volume  $V = 4.63 \text{ cm}^3/\text{mol}$ ; coefficient of the linear thermal dilatation  $\alpha = 8.29 \cdot 10^{-6} \text{ K}^{-1}$  between 20 and  $750^\circ\text{C}$ ) [42]; reciprocal cubic compressibility  $B = 1.78 \cdot 10^{12} \text{ erg cm}^{-2}$ ,  $C_p = 1.21 \cdot 10^8 \text{ erg/mol K}$  [43]) a medium Grüneisen constant

$$G = 3\alpha BV/C_V = 1.85$$

( $C_V = C_p - 9\alpha^2 BV T$ ) can be obtained. With  $dV = V 3\alpha dT$  and  $G = -V(\partial\omega_i/\partial V)_T/\omega_i$  the frequency shift of the phonons results:

$$\omega_i(T_2) - \omega_i(T_1) = \int_{T_1}^{T_2} \omega_i G 3\alpha(T) dT.$$

If a frequency and temperature independent Grüneisen constant and a temperature independent thermal dilatation coefficient is assumed, one gets

$$\begin{aligned} \frac{\omega_i(T_2) - \omega_i(T_1)}{\omega_i(T_1)} &= -G 3\alpha(T_2 - T_1) = \\ &= -4.6 \cdot 10^{-5} (T_2 - T_1). \end{aligned}$$

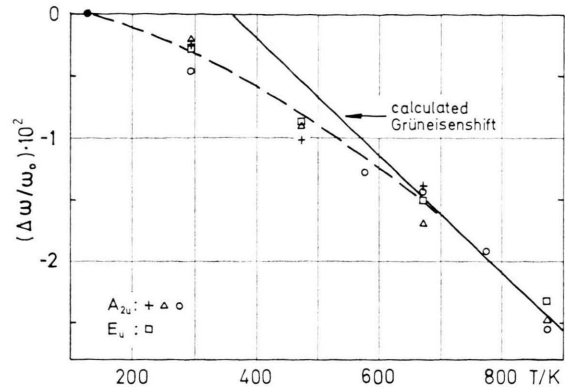


Fig. 11. Frequency shift of some phonons of  $\beta$ -boron depending on temperature in comparison with the calculated Grüneisen shift.

Figure 11 shows the experimental results of the frequency shift of some phonons of both species plotted in comparison with the calculated Grüneisen shift. At high temperatures the agreement is good. Within the accuracy of measurement no anisotropy could be detected.

The temperature dependence of the damping constant of the phonons in a crystal has been determined by Sakurai and Sato [41] to be

$$\begin{aligned} \gamma_i &= a \left\{ \left( \exp \frac{\hbar\omega_i}{2kT} - 1 \right)^{-1} + 1/2 \right\} + \\ &+ b \left\{ \left[ \left( \exp \frac{\hbar\omega_i}{2kT} - 1 \right)^{-1} + 1/2 \right]^2 + 1/12 \right\}. \end{aligned}$$

Herein the first term describes three-phonon processes and the second one four-phonon processes with energy dissipation by transitions into phonons of equal partial energy respectively. As seen in Fig. 12 the consideration of both processes is necessary for a satisfying description of the experimental results.

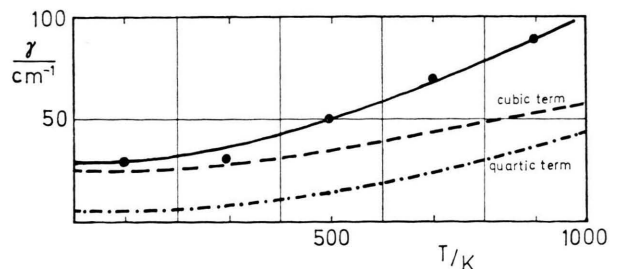


Fig. 12. Damping constant of the  $1250/1275 \text{ cm}^{-1}$  phonon of  $\beta$ -boron; ---- three-phonon processes, - · - four phonon processes, — three-phonon and four-phonon processes (theoretical curves fitted by use of  $a = 50$  and  $b = 15 \text{ cm}^{-1}$ ).

### Acknowledgements

The authors would like to thank Prof. Happ for supporting parts of this work. They are indebted to the Wacker-Chemie, Munich, especially to Dr. Kölker for supplying the boron crystals and to the

Elektroschmelzwerk Kempten, especially to Dr. Schwetz for supplying the boron carbide. Parts of the work have been supported by the government of Northrhine-Westfalia and by the Deutsche Forschungsgemeinschaft.

- [1] H. J. Becher, *Z. Anorg. Chem.* **321**, 317 (1960); *Boron*, Vol. 2, Ed. G. K. Gaulé, Plenum Press, New York 1964, p. 89.
- [2] W. Richter, A. Hausen, and H. Binnenbruck, *phys. stat. sol. (b)* **51**, 115 (1972).
- [3] W. Weber and M. F. Thorpe, *J. Phys. Chem. Solids* **36**, 967 (1975).
- [4] W. Richter, W. Weber, and K. Ploog, *J. less-comm. met.* **47**, 85 (1976).
- [5] H. Binnenbruck and H. Werheit, *J. less-comm. met.* **47**, 91 (1976).
- [6] H. Werheit, Die Halbleitereigenschaften des Bors, in: *Festkörperprobleme X*, Ed. O. Madelung, Vieweg, Braunschweig 1970, p. 189 (references on earlier papers therein).
- [7] H. Werheit, A. Hausen, and H. Binnenbruck, *phys. stat. sol.* **42**, 733 (1970).
- [8] H. Werheit, H. Binnenbruck, and A. Hausen, *phys. stat. sol. (b)* **47**, 153 (1971).
- [9] H. Werheit, A. Hausen, and H. Binnenbruck, *phys. stat. sol. (b)* **51**, 115 (1972).
- [10] E. L. Muetterties, in: *General Introduction to Boron Chemistry*; Ed. E. L. Muetterties, Wiley & Sons, New York 1967.
- [11] B. Sullenger, Ch. L. Kennard, *Sci. Amer.* **215**, No. 7, 96 (1966).
- [12] J. L. Hoard, in: *Boron*, Vol. 1, Ed. J. A. Kohn, W. F. Nye, and G. K. Gaulé, Plenum Press, New York 1960, p. 1.
- [13] H. L. Longuet-Higgins and M. de V. Roberts, *Proc. Roy. Soc. London* **230A**, 110 (1955).
- [14] R. Hoffmann and W. N. Lipscomb, *J. Chem. Phys.* **36**, 2181 (1962).
- [15] B. F. Decker and J. S. Kasper, *Acta Cryst.* **12**, 503 (1959).
- [16] J. L. Hoard, R. E. Hughes, in: *General Introduction to Boron Chemistry*; Ed. E. L. Muetterties, Wiley & Sons, New York 1966.
- [17] V. J. Matkovich, *J. less-comm. met.* **47**, 39 (1976).
- [18] G. Will and K. H. Kossobutzki, *J. less-comm. met.* **47**, 43 (1976).
- [19] A. Lipp, *Tech. Rdsch.* **57**, No. 14, 5 (1965); **57**, No. 28, 19 (1965); **57**, No. 33, 5 (1965); **58**, No. 7, 3 (1966).
- [20] H. Werheit, *Boron*, Vol. 6 (in the press).
- [21] R. Naslain, in: *Boron and Refractory Borides*; Ed. V. J. Matkovich, Springer-Verlag, Berlin, Heidelberg, New York 1977, p. 139.
- [22] J. L. Hoard, R. E. Hughes, C. H. L. Kennard, D. B. Sullenger, H. A. Weahlim, and D. E. Sands, *J. Amer. Chem. Soc.* **85**, 361 (1963).
- [23] P. Runow, *J. Mat. Sci.* **7**, 499 (1972).
- [24] H. Binnenbruck, A. Hausen, P. Runow, and H. Werheit, *Z. Naturforsch.* **25a**, 1431 (1970).
- [25] K. Mathiak and P. Stingl, *Gruppentheorie*, Vieweg (Akad. Verl.-Ges.), Braunschweig 1968.
- [26] F. Matossi, *Gruppentheorie der Eigenschwingungen von Punktsystemen*, Springer-Verlag, Berlin 1961.
- [27] M. Tinkham, *Group Theory and Quantum Mechanics*, McGraw-Hill Book-Comp., New York 1964.
- [28] H. Werheit, unpublished results.
- [29] S. S. Mitra, *Optical Properties of Solids*, Ed. S. Nudelman and S. S. Mitra, Plenum Press, New York 1969, p. 358.
- [30] J. T. Houghton and S. D. Smith, *Infrared Physics*, Clarendon Press, Oxford 1966.
- [31] H. Bilz, L. Genzel, and H. Happ, *Z. Phys.* **160**, 535 (1960).
- [32] H. Werheit, A. Hausen, and H. Binnenbruck, *phys. stat. sol.* **42**, K 57 (1970).
- [33] J. Lagrenaudie, *J. Chim. Phys.* **50**, 629 (1953).
- [34] D. Geist, J. Meyer, and H. Preußner, in: *Boron*, Vol. 3, Ed. T. Niemyski, Polish Scientific publishers, Warsaw 1970.
- [35] H. Werheit and K. de Groot, to be published.
- [36] W. Zimmerman, A. M. Murphy, and C. Feldman, *Appl. Phys. Letters* **10**, 71 (1967).
- [37] G. A. Slack, D. W. Oliver, and F. H. Horn, *Phys. Rev. B* **4**, 1714 (1971).
- [38] K. Katada, *J. Appl. Phys.* **5**, 582 (1966).
- [39] J. Jaumann and H. Werheit, *phys. stat. sol.* **33**, 587 (1969).
- [40] R. F. Wallis, I. P. Ipatova, and A. A. Maradudin, *Sov. Phys. Solid State* **8**, 850 (1966); I. P. Ipatova, A. A. Maradudin, and R. F. Wallis, *Phys. Rev.* **155**, 882 (1967).
- [41] T. Sakurai and T. Sato, *Phys. Rev. B* **4**, 583 (1971).
- [42] D'Ans-Lax, *Taschenbuch für Chemiker und Physiker*, Springer-Verlag, Berlin 1967.
- [43] S. S. Wise, J. L. Margrave, and R. L. Altman, *J. Phys. Chem.* **64**, 915 (1960).